Effects of Precipitate Element Addition on Microstructure and Magnetic Properties in Magnetostrictive Fe$_{83}$Ga$_{17}$ alloy

Jiheng Li*, Chao Yuan, Wenlan Zhang, Xiaoqian Bao, and Xuexu Gao

State Key Laboratory for Advanced Metals and Materials, University of Science and Technology Beijing, Beijing 100083, China

The <100> oriented Fe$_{83}$Ga$_{17}$ alloys with various contents of NbC or B were prepared by directionally solidification method at the growth rate of 720 mm·h^{-1}. With a small amount of precipitates, the columnar grains grew with cellular mode during directional solidification process, while like-dendrite mode of grains growth was observed in the alloys with higher contents of 0.5 at% due to the dragging effect of precipitates on the boundaries. The NbC precipitates disperse both inside grains and along the boundaries of Fe$_{83}$Ga$_{17}$ alloys with NbC addition, and the Fe$_2$B secondary phase particles preferentially distribute along the grain boundaries in B-doped alloys. Precipitates could affect grain growth and improved the <100> orientation during directional solidification process. Small amount of precipitate element addition slightly increased the magnetostrictive strain, and a high value of 335 ppm under pre-stress of 15 MPa was achieved in the alloys with 0.1 at% NbC. Despite the fact that the effect on magnetic induction density of small amount of precipitates could be negligible, the coercivity markedly increased with addition of precipitate element for Fe$_{83}$Ga$_{17}$ alloy due to the retarded domain motion resulted by precipitates.

Keywords : magnetostriction, Fe-Ga alloy, niobium carbide, boron, microstructure, magnetic property

1. Introduction

Magnetostrictive Fe-Ga alloys, also named "Galfenol", have received increasing attention as a new magnetostrictive smart material for actuator, sensor, and energy harvesting applications [1, 2]. This interest stems from facts that unlike existing smart material systems, Galfenol is the first to offer the combination of good magnetostrictive properties and mechanical properties. Magnetically [3], the addition of Ga increases the magnetostrictive capability of Fe over tenfold up to 400 ppm (3/2 λ_{100}) along <100> direction in single crystal material. Mechanically [4], Fe-Ga alloys are strength (> 500 MPa) and robust not exhibited by materials such as PZT, PMN, or Terfenol-D. In addition, Fe-Ga alloys have high permeability (μ_r > 100) [5], high Curie temperature (T$_c$ > 650 °C) [6] and low temperature dependence (~0.5 ppm/°C) [7]. This combination of magnetic and mechanical properties makes Fe-Ga alloy a unique material.

The high conductivity of Fe-Ga alloy requires its form of thin sheet to avoid eddy current losses. Efforts have been made to get thin sheets by rolling process [8-10]. However, the polycrystalline Fe$_{81}$Ga$_{19}$ binary alloy cracked and fractured along grain boundaries during hot rolling and was too brittle to make thin sheets. Subsequently, it has been reported that small addition of precipitate elements of NbC and B, substitutional elements of V, Cr, Mo and Nb, could improved the ductility of polycrystalline Fe-Ga alloys for plastic working [11]. As well known, the dispersion of NbC or Fe$_2$B precipitates could refine grain size and pin dislocations, which results in the inhibition of intergranular fracture and the enhancement of mechanical properties. On the other hand, precipitates of NbC or Fe$_2$B acting as inhibitors which resulted in abnormal grain growth (AGG) have promoted the developing of Cubic texture {100}<001> or Goss texture {110} <001> in the Fe-Ga rolled sheets [12, 13]. Cubic or Goss texture play an important role in achieving high magnetostrictive performance due to the anisotropic nature of the magnetostriction in the Fe-Ga rolled sheets. For single crystal Fe-Ga alloy, the trace amounts of interstitial atoms, such as C, B and N, can improve the magnetostriction [14]. But, in almost all cases, ternary additions, such as substitutional elements of V, Cr, Mn, Co, Rh, Ni,

*Corresponding author: Tel: +86-10-62333502
Fax: +86-10-62332508, e-mail: lijiheng628@163.com

Mo, and Al, have decreased the magnetostriction values from the binary Fe-Ga single crystal [15]. The beneficial influences of precipitate of Fe_2B and NbC on the mechanical properties and texture evolution in rolled Fe-Ga alloy sheet have drawn much attention, but little attention was paid to their influence on microstructure and intrinsical magnetic properties of directional solidified Fe-Ga alloys.

In this work, directional solidified (DS) Fe-Ga alloys with low levels addition of NbC or B were investigated. Preferred <100> grain orientation was obtained at a growth rate of 720 mm·h^{-1}. A slight improvement in the magnetostrictive performance under pre-stress was observed for the Fe-Ga alloys with small amount of NbC and B addition, and the highest magnetostriction above 300 ppm was achieved. The influence on intrinsical magnetic properties, such as B (magnetic induction density) and H_c (the coercivity), was also discussed.

2. Experimental

$Fe_{83}Ga_{17}$-based alloys with 0, 0.1, 0.2, 0.5 at% NbC or 0.2, 0.5 at% B were prepared from pure-Fe (99.9%), Ga (99.99%), and master alloys of Nb-Fe, Fe-C and Fe-B. Excess Ga of 2-3% total Ga content was used to account for the Ga loss during induction melting. The oriented alloy rods with 30 mm diameter and 100 mm length were produced by directional solidification. A new method of directional solidification was employed. The raw material was molten in induction melting system, and then the molten metal was drawn into a quartz tube placed previously in the holding furnace with a given temperature
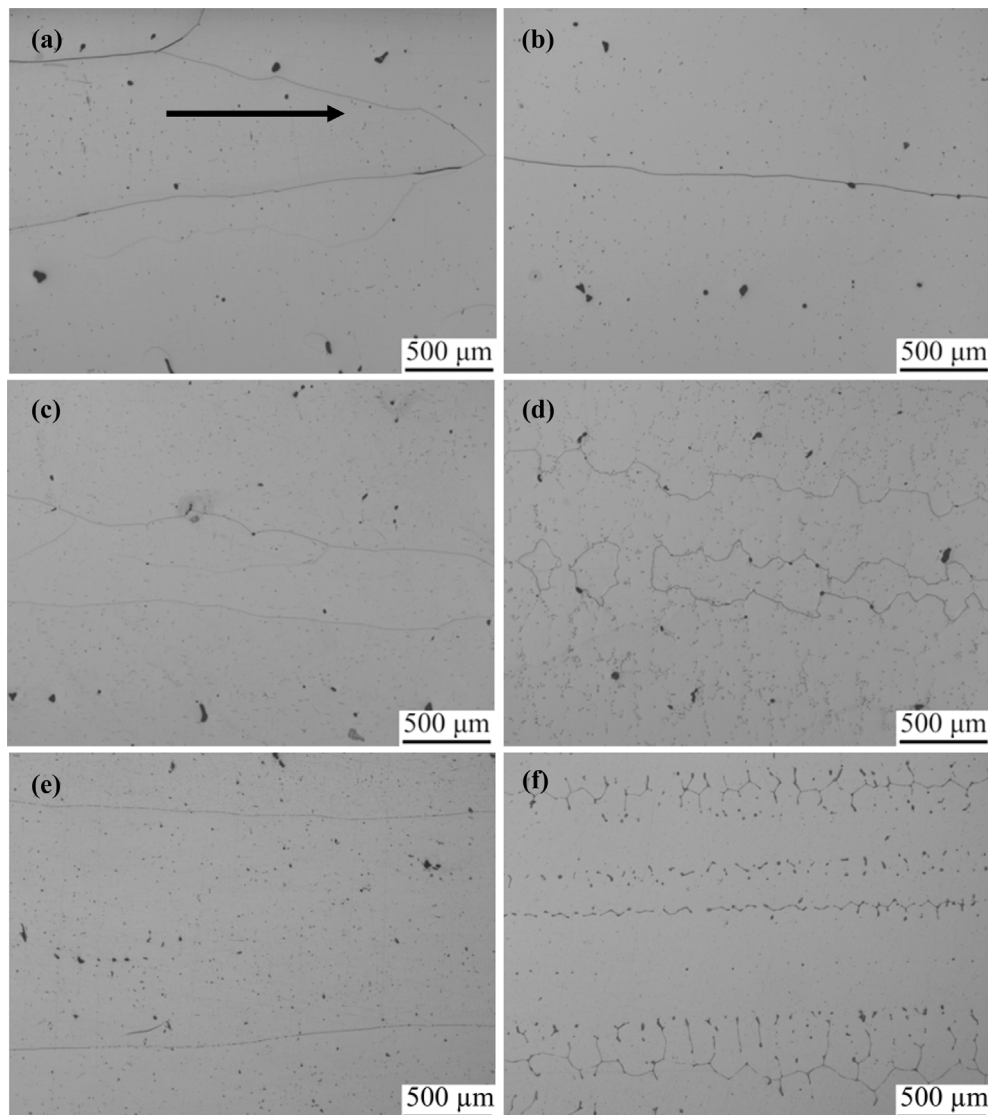

Fig. 1. Optical photographs along the growth direction: (a)$Fe_{83}Ga_{17}$; (b) $Fe_{83}Ga_{17}$+0.1 at% NbC; (c) $Fe_{83}Ga_{17}$+0.2 at% NbC; (d) $Fe_{83}Ga_{17}$+0.5 at% NbC; (e) $Fe_{83}Ga_{17}$+0.2 at% B; (f) $Fe_{83}Ga_{17}$+0.5 at% B. The arrows show the growth direction of alloys.

gradient (about 55 K/cm). After pouring, the tube was moved down with rate of 720 mm·h^{-1} by motor immediately. All the rods were annealed at 1,100 °C for 1 h, and then furnace cooled to 730°C and held for 3 h, followed by water quenching to room temperature.

The phase of the samples was detected using X-ray diffraction (XRD). Micro-structure and precipitates were examined by optical microscopy, scanning electron microscopy (SEM) and energy dispersive X-ray spectroscopy (EDS). Electron backscattering diffraction (EBSD) patterns were captured from scanning area of ~4 × 3 mm^2 on the cross section, and analyzed to obtain inverse pole figure (IPF). The magnetostriction under different prestress was measured by strain gauge along the growth direction, and the measured position was on the middle position of the rods. Room-temperature magnetic hysteresis loops were examined by NIM-2000S soft magnetic mea-

surement system in an applied magnetic field of 8,000 A·m^{-1}. The samples shape for magnetic measurements is ring with size of Ø28 × Ø22 × 5 mm.

3. Results and Discussion

The longitudinal optical microstructures of Fe-Ga alloys with various NbC and B contents are shown in Fig. 1, and the arrow shows the growth direction of rods. From the optical photographs, it can be found that the grain growth direction is approximately parallel to the solidification direction (also known as axial direction of rod), and the size of a single columnar crystal could be up to several millimetre. Obviously, the grain boundaries are flat in the alloys with addition of either NbC or B less than 0.2 at%, indicating the columnar grains grew with cellular mode during directional solidification process. But, the grain
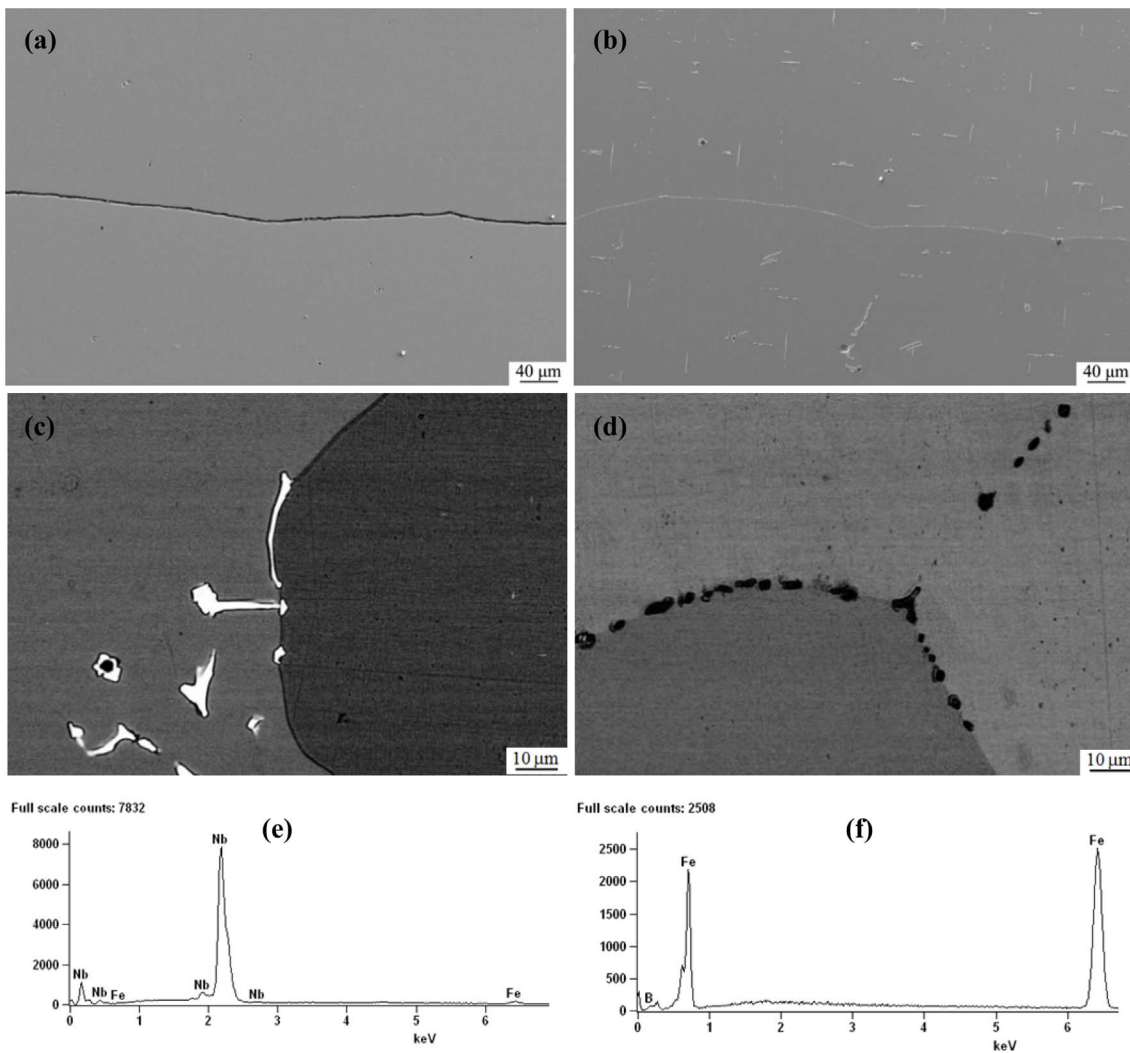

Fig. 2. SEM photographs (a) Fe$_{83}$Ga$_{17}$+0.1 at% NbC; (b) Fe$_{83}$Ga$_{17}$+0.2 at% NbC; BSE photographs and EDS profiles of precipitates: (c), (e) Fe$_{83}$Ga$_{17}$+0.5 at% NbC; (d), (f) Fe$_{83}$Ga$_{17}$+0.5 at% B.

boundaries become greatly curved at higher contents of 0.5 at%, which could be attributed to the dragging effect of precipitates on the boundaries. In addition, it can be seen that large amount of precipitates uniformly distribute in the alloys with NbC or B content of 0.5 at%. For NbC addition, the precipitates disperse both inside grains and along the boundaries, while the precipitates mainly distribute along the grain boundaries in B-doped alloys. Scanning electron microscopy (SEM) and energy dispersive X-ray spectroscopy (EDS) were employed to further identification of precipitates. Figure 2 shows the SEM and BSE (backscattered electron) photographs of the alloys with NbC or B addition. Very few tiny Nb-rich precipitates can be found in the alloy with 0.1 at% NbC, as shown in Fig. 2(a). With the increase of NbC content, many bar-shaped precipitates can be observed in the matrix (Fig. 2(b)), and the amount of precipitates greatly increases for the 0.2 at% NbC doped alloys. It can be seen from Fig. 2(c) and (e) that a lot of tiny Nb-rich precipitates, less than 5 μm and a few with bar-shaped, can be observed both inside grains and along the boundaries of $Fe_{83}Ga_{17}$-0.5 at% NbC alloy. Nb atom has a low solubility in the α-Fe and tends to precipitate with C, N atoms in metal alloys, resulting in a large amount of Nb-rich precipitates with high NbC contents. The results shown in Fig. 2(b) and (f) demonstrate that there are many B-rich precipitates distributed along the gain boundaries and the matrix alloy is homogeneous, which indicates that the element of B was preferentially segregated at grain boundaries in 0.5 at% B-doped $Fe_{83}Ga_{17}$ alloys.

The XRD patterns captured from the cross section on the middle position of the rods are shown in Fig. 3. In the XRD patterns, (110) peaks often appear as the strongest peak for bcc metals with randomly orientation. It can be seen from Fig. 3(a) that (200) peaks dominate the patterns in all directional solidified samples, rather than the (110) peaks, which indicates the preferred (100) orientation along the growth direction. Interestingly, compared with binary Fe-Ga alloy, the relative diffraction intensity of (200) to (110) notably increases with the addition of NbC or B, suggesting the introduction of precipitates may favor the development of (100) orientation during the DS process. Also, very weak peaks corresponding to NbC at ~40.29° and ~58.3° can be found in 0.2 at% and 0.5 at% NbC doped alloy, meanwhile some peaks at ~34.91°, ~42.34° and ~44.83° from Fe_2B precipitate shown in the inset were detected in the alloy with 0.5 at% B addition, which agrees with the microstructure observed in Fig. 1 and 2. On the other hand, the shift of the XRD peaks to the left of the pattern of the binary alloy is shown in Fig. 3(b), which indicated an expansion of the lattice parameter of Fe-Ga alloy with 0.1 at% NbC addition. Additionally, a small peak around 30.7° corresponding to the DO_3 structure appears to be unexpected, which could be attributed to the low temperature gradient (about 55 K/cm) and the increased DO_3 stabilization. A trace amount of interstitial atoms C and B or substitutional atom Nb into the Fe-Ga alloy matrix are known to produce a tetragonal distortion and increase the stabilization of DO_3. The electron/atom ratios of ternary atoms on different sites of the DO_3 structure could be less than the average Fe_3Ga electron/atom ratio reside on the mixed simple cubic lattice (Fe I) and atoms with electron/atom ratios greater than the Fe_3Ga electron/atom ratio reside on the pure iron sublattice (Fe II) [16, 17].

To obtain the exact orientation information, orientation maps and their corresponding IPFs on the cross section of
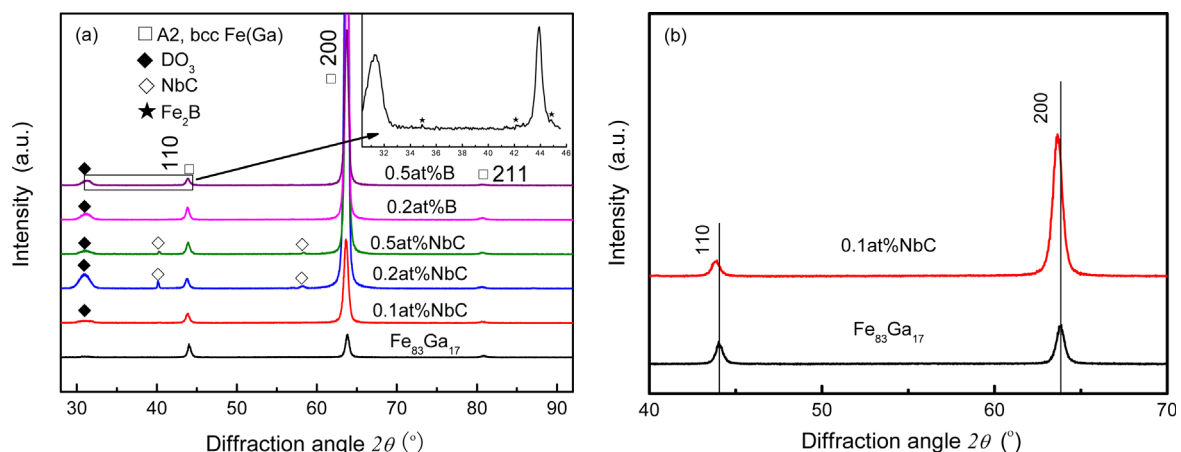

Fig. 3. (Color online) XRD patterns on the cross section of the directional solidified $Fe_{83}Ga_{17}$ alloys with addition of NbC and B, (a); Partially enlarged XRD, (b).
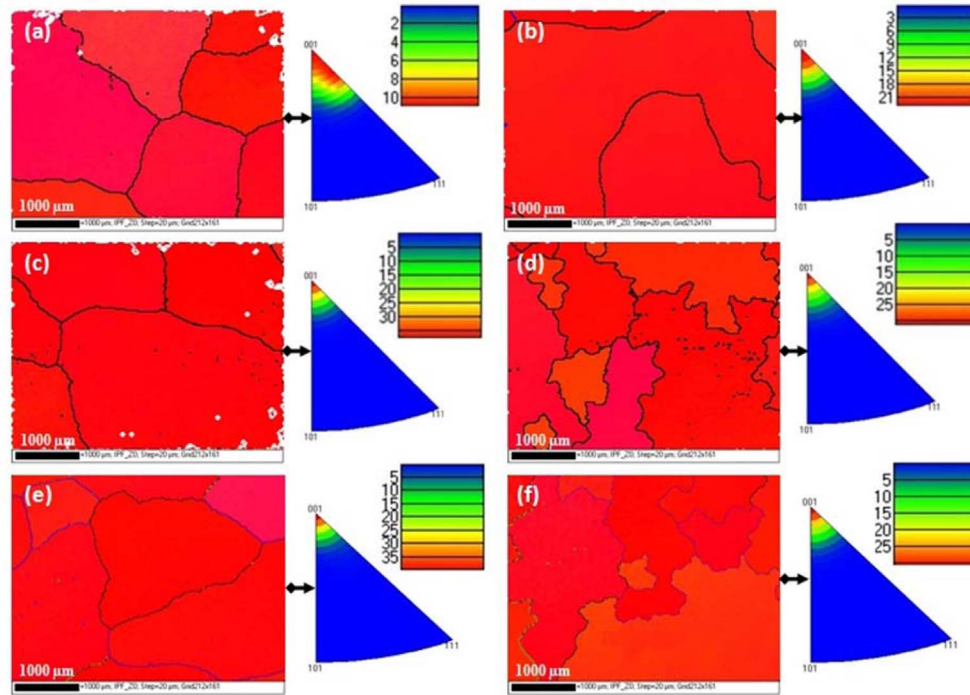
Fig. 4. (Color online) Orientation maps and their corresponding IPFs on the cross section of the samples: (a) $Fe_{83}Ga_{17}$; (b) $Fe_{83}Ga_{17}$+0.1 at% NbC; (c) $Fe_{83}Ga_{17}$+0.2 at% NbC; (d) $Fe_{83}Ga_{17}$+0.5 at% NbC; (e) $Fe_{83}Ga_{17}$+0.2 at% B; (e) $Fe_{83}Ga_{17}$+0.5 at% B.

growth direction were captured, as shown in Fig. 4. In orientation maps, grains with <001> orientation growth direction to within 15° are colored red. From the IPFs, it can be found that all the samples exhibit the preferred <100> orientation, consistent with the dominant {200} diffraction peak in the XRD patterns. Though all the alloys exhibit very close <100> orientation, a slight improvement of orientation degree in the NbC or B doped alloys can be observed obviously compared with that of binary alloy. It is considered that the improvement of the

preferred orientation is related to the influence of addition element on growth behavior of the solid-liquid interface at the solidification front. On the other hand, during directional solidification process, the pinning effect on grain boundaries of secondary phase particles, reduced grain boundary active and migration. As a result, the smaller misorientation between columnar grains could be achieved in NbC or B doped alloys. The possibility that the segregated B may increase the fraction of low angle boundaries and improve the orientation degree has also
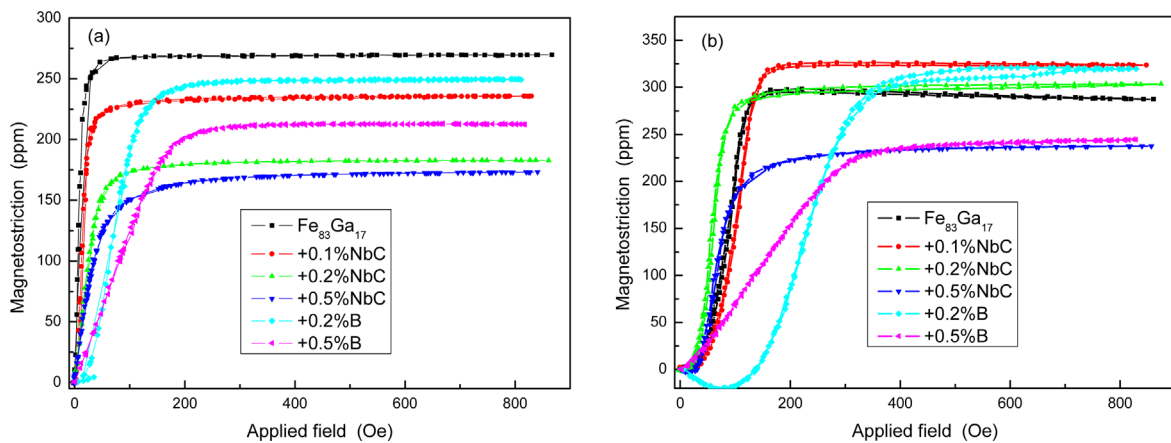

Fig. 5. (Color online) Magnetostrictive curves versus applied magnetic field of the directional solidified $Fe_{83}Ga_{17}$ alloys with addition of NbC and B: (a) 0 MPa; (b) 15 MPa.

Table 1. Magnetostriction of the directional solidified Fe_{83}-Ga_{17} alloys with addition of NbC and B under different pre-stress.

Composition	Magnetostriction (ppm) under pre-stress			
	0 MPa	5 MPa	10 MPa	15 MPa
Binary alloy	269	286	294	300
0.1 at.% NbC	235	302	326	335
0.2 at.% NbC	183	277	303	311
0.5 at.% NbC	173	221	237	241
0.2 at.% B	250	300	318	336
0.5 at.% B	208	245	252	264

been considered in Ni_3Al alloys [18, 19], and Farkas et al. have pointed out that B significantly increased low angle boundaries from less than 9% in B-free alloys up to 26% in B-doped Ni-24.8Al alloys [19].

The axial magnetostriction of Fe-Ga alloy rods parallel to external magnetic field were measured at the middle position along the growth direction. The room temperature magnetostrictive curves versus applied field under different pre-stress are shown in Fig. 5. Without pre-stress employed, the saturation magnetostriction is as high as 269 ppm for the $Fe_{83}Ga_{17}$ alloy, but some decreases are observed with NbC or B addition, as shown in Fig. 5(a). When pre-stress was applied, the maximum value appeared in the $Fe_{83}Ga_{17}$ alloys with 0.1 at% NbC, and the saturation magnetostriction can be as high as 335 ppm under 15 MPa pre-stress. With a little higher NbC content (0.2 at%), the saturation magnetostriction value slightly decreases. But, there is an obvious decrease of magnetostriction with further increasing the NbC content to 0.5 at%, as shown in Fig. 5(b). Similar change trend of saturation magnetostriction was observed in B-doped alloys. The maximum measured magnetostriction of $Fe_{83}Ga_{17}$ alloys with NbC or B additions under different pre-stress are shown in Table 1.

The magnetostriction is closely related to the composition and microstructure in Fe-Ga alloys. Clark *et al.* [14, 17] have discovered that the additions of trace amounts of small interstitial atoms C and B to Fe-Ga alloys have beneficial effect on the magnetostriction of Fe-Ga alloys. Interstitial atom C or substitutional atom Nb in $Fe_{83}Ga_{17}$ alloy produced a tetragonal distortion, as shown in Fig. 3(b), and such tetragonal distortions are thought to contribute to increased magnetostriction. Combined with the stronger <100> orientation (Fig. 4(b)) and uniform and clean microstructure (Fig. 2(a)), higher magnetostriction was obtained in the alloys with small amount of NbC addition than that in binary alloy. The decrease in the magnetostriction of alloys with higher

NbC contents could be mainly ascribed to the large amount of precipitates distributed inside grains which could affect the magnetic domain structure of matrix alloy. Under no pre-stress, the lower magnetostriction in the 0.1 at% NbC-doped alloy maybe attributed to the less domain assignment than that in binary alloys, due to the pinning effect of non-magnetic particles. Under saturation pre-stress, the domains are well assigned perpendicular to the pre-stress direction, and fully rotate to the magnetic field direction under the saturation magnetic field, thus larger magnetostriction is obtained under pre-stress. As for B-doped alloys, a similar explanation could be gotten. Additionally, Fe_2B precipitates distributed along grain boundaries could result in an increase of Ga content of matrix alloy, which maybe also thought to contribute to increased magnetostriction. In addition, the observed ordered phase DO_3 in the XRD results can also affect the magnetostriction [20].

Compared with that of binary Fe-Ga alloy, the $d\lambda/dH$ of NbC-doped alloys without pre-stress gradually decreased with NbC addition, meanwhile there are a marked decrease in B-doped alloy, as shown in Fig. 6. The $d\lambda/dH$ is of great importance for the practical application, and lower $d\lambda/dH$ means higher applied field magnetic field is needed for the same level of magnetostrictive strain. As well known, the non-magnetic particles in the ferromagnetic materials can retard the domain walls, thus higher energy, such as magnetic field or pre-stress, is needed for the domain motion. There is large number of secondary phase particles in the alloys with high NbC or B addition, and this is the main reason for the lower $d\lambda/dH$.

Magnetic hysteresis loops was examined in an applied magnetic field of 8,000 $A \cdot m^{-1}$ at room temperature. The results shown in Fig. 7 and Table 2 suggest that precipitate elements addition of NbC or B slightly reduce the
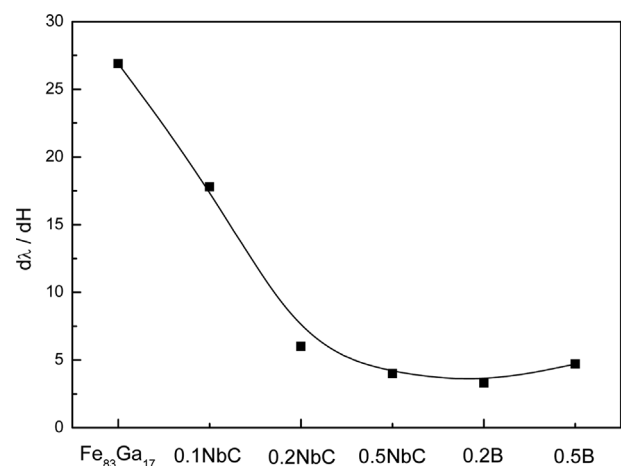
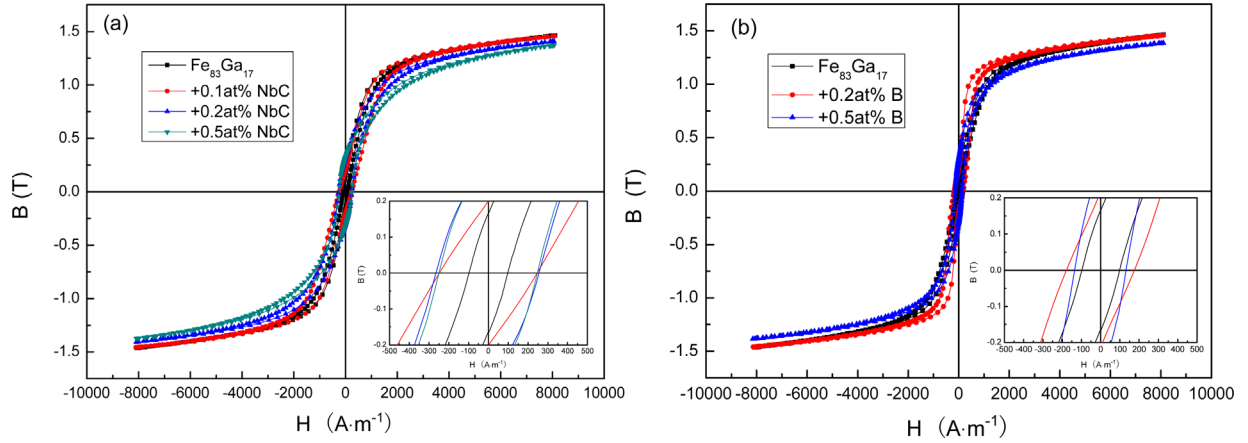**Fig. 6.** The variations of $d\lambda/dH$ with precipitate element additions.

Fig. 7. (Color online) Room temperature magnetic hysteresis loops of the directional solidified $Fe_{83}Ga_{17}$ alloys with precipitate element addition: (a) NbC; (b) B.

Table 2. Magnetic properties of the directional solidified $Fe_{83}Ga_{17}$ alloys with addition of NbC and B.

Composition	B (T)	H_c (A/m)
Binary alloy	1.507	87
0.1 at.% NbC	1.485	190
0.2 at.% NbC	1.438	217
0.5 at.% NbC	1.422	213
0.2 at.% B	1.491	133
0.5 at.% B	1.418	106

magnetic induction density B, while obviously increase the coercivity H_c of $Fe_{83}Ga_{17}$ alloy. The non-magnetic NbC particles in the $Fe_{83}Ga_{17}$ alloy could retard the domain walls and consequently higher energy is needed for the domain motion, resulting in a significant increase of the coercivity. The magnetic moment of Fe_2B precipitates is different from the matrix, which will impede the movement of the domain wall and increase the coercivity. The increase of the coercivity is not proportional to the number of the secondary phases because of their different sizes and distributions. It is noteworthy that the increase rate of the coercivity for NbC-doped alloy is remarkably larger than that of alloys with B addition due to the pinning effect of NbC precipitates dispersed inside grains on domain motion of matrix alloy. As compared, the resistance to movement of the magnetic domains is much smaller for B-added alloys, because Fe_2B particles mainly distributed along the grain boundaries.

4. Conclusion

The <100> oriented $Fe_{83}Ga_{17}$-based alloys with addition of 0, 0.1, 0.2, 0.5 at% NbC or 0.2, 0.5 at% B were prepared by directional solidification method at the growth rate of

720 mm·h^{-1}. With a small amount of precipitates, the columnar grains grew with cellular mode during directionally solidification process, while like-dendrite mode of grains growth was observed in the alloys with higher contents of 0.5 at% due to the dragging effect of precipitates on the boundaries. The NbC precipitates disperse both inside grains and along the boundaries, and the Fe_2B particles preferentially distribute along the grain boundaries. Precipitates could affect grain growth and improve the <100> orientation during the DS process. Small amount of precipitate element addition less than 0.2 at% slightly increased the magnetostrictive strain, and a high value of 335 ppm under pre-stress of 15 MPa was achieved in the alloys with 0.1 at% NbC. Despite the fact that the effect on magnetic induction density B of small amount of precipitates could be negligible, the coercivity H_c increased remarkably with addition of precipitate element for $Fe_{83}Ga_{17}$ alloy.

References

[1] S. Guruswamy, N. Srisukhumbowornchai, A. E. Clark, J. B. Restorf, and M. Wun-Fogle, Scr. Mater. **43**, 239 (2000).

[2] A. E. Clark, J. B. Restorff, M. Wun-Fogle, T. A. Lograsso, and D. L. Schlagel, IEEE Trans. Magn. **36**, 3238 (2000).

[3] A. E. Clark, K. B. Hathaway, M. Wun-Fogle, J. B. Restorff, T. A. Lograsso, V. M. Keppens, G. Petculescu,

and R. A. Taylor, J. Appl. Phys. **93**, 8621 (2003).

[4] R. A. Kellogg, A. M. Russell, T. A. Lograsso, A. B. Flatau, A. E. Calrk, and M. Wun-Fogle, Acta Mater. **52**, 5043 (2004).

[5] A. E. Clark, M. Wun-Fogle, J. B. Restorf, T. A. Lograsso, and J. R. Cullen, IEEE Trans. Magn. **37**, 2678 (2001).

[6] A. E. Clark, M. Wun-Fogle, J. B. Restorf, and T. A. Lograsso, Mater. Trans. **43**, 881 (2002).

[7] R. A. Kellogg, A. B. Flatau, A. E. Clark, M. Wun-Fogle, and T. A. Lograsso, J. Appl. Phys. **91**, 7821 (2002).

[8] L. M. Cheng, A. E. Nolting, B. Voyzelle, and C. Galvani, Proc. SPIE. 6526, 65262N (2007).

[9] S. M. Na and A. B. Flatau, J. Appl. Phys. **101**, 09N518 (2007).

[10] E.M. Summers, R. Meloy, and S. M. Na, J. Appl. Phys. **105**, 07A922 (2009).

[11] S. M. Na and A. B. Flatau, J. Appl. Phys. **103**, 07D304 (2008).

[12] J. H. Li, X. X. Gao, J. Zhu, X. Q. Bao, T. Xia, and M. C. Zhang, Scr. Mater. **63**, 246 (2010).

[13] S. M. Na and A. B. Flatau, Scr. Mater. **66**, 307 (2012).

[14] M. L. Huang, T. A. Lograsso, A. E. Clark, J. B. Restorff, and M. Wun-Fogle, J. Appl. Phys. **103**, 07B314 (2008).

[15] E. M. Summers, T. A. Lograsso, and M. Wun-Fogle, J. Mater. Sci. **42**, 9582 (2007).

[16] N. Kawamiya and K. Adachi, J. Magn. Magn. Mater. **31-34**, 145 (1983).

[17] A. E. Clark, J. B. Restorff, M. Wun-Fogle, K. B. Hathaway, T. A. Lograsso, M. Huang, and E. Summers, J. Appl. Phys. **101**, 09C507 (2007).

[18] A. Chiba, S. Hanada, S. Watanabe, T. Abe, and T. Obana, Acta Metall. Mater. **42**, 1733 (1994).

[19] D. Farkas, H. Jang, and M. O. Lewus, Mat. Res. Symp. Proc. **122**, 455 (1988).

[20] S. Datta, M. Huang, J. Raim, T. A. Lograsso, and A. B. Flatau, Mat. Sci. Eng. A. **435-436**, 221 (2006).